

Generation and optimization of entanglement between giant atoms chirally coupled to spin cavities

Jia-Bin You^{1,*}, Jian Feng Kong¹, Davit Aghamalyan¹, Wai-Keong Mok², Kian Hwee Lim³, Jun Ye¹, Ching Eng Png¹ and Francisco J. García-Vidal^{1,4,†}

¹*Institute of High Performance Computing (IHPC), Agency for Science, Technology and Research (A*STAR), 1 Fusionopolis Way, #16-16 Connexis, Singapore 138632, Republic of Singapore*

²*Institute for Quantum Information and Matter, California Institute of Technology, Pasadena, CA 91125, USA*

³*Centre for Quantum Technologies, National University of Singapore, 3 Science Drive 2, Singapore 117543*

⁴*Departamento de Física Teórica de la Materia Condensada and Condensed Matter Physics Center (IFIMAC), Universidad Autónoma de Madrid, E-28049 Madrid, Spain*

We explore an scheme for entanglement generation and optimization in giant atoms by coupling them to finite one-dimensional arrays of spins that behave as cavities. We find that high values for the concurrence can be achieved in small-sized cavities, being the generation time very short. When exciting the system by external means, optimal concurrence is obtained for very weak drivings. We also analyze the effect of disorder in these systems, showing that although the average concurrence decreases with disorder, high concurrences can still be obtained even in scenarios presenting strong disorder. This result leads us to propose an optimization procedure in which by engineering the on-site energies or hoppings in the cavity, concurrences close to 1 can be reached within an extremely short period of time.

Introduction.— Entanglement is a vital resource for various quantum information technologies, such as quantum teleportation [1], quantum key distribution [2, 3], and quantum computing [4]. Researchers have been actively working to develop techniques for generating and optimizing entanglement in a variety of physical systems, such as plasmonic structures [5], cavity quantum electrodynamics (QED) setups [6], and circuit-QED platforms [7]. One of the key figures of merit for entanglement generation is to maximize the entanglement while minimizing the generation time [8–10]. In recent years, chiral light-matter interaction has turned out to be a promising ingredient [11–14] for generating non-classical states of light [15] and entangled states, and several theoretical studies have shown that fully chiral systems can significantly boost dynamical entanglement generation [16, 17] and both quantum state [17, 18] and entanglement transfer [18]. Chirality appears as a natural manifestation of spin-orbit coupling of light [12], as demonstrated in seminal experiments with atoms and quantum dots coupled to photonic nanostructures [14, 19–23].

An emerging platform displaying chiral light-matter coupling has been built using giant atoms coupled to either structures supporting surface acoustic waves [24–26] or microwave waveguides [27–30]. Importantly, giant atoms can interact with a waveguide at multiple points such that this nonlocal coupling can enable quantum interference effects, leading to nonzero hopping phase that is essential in our scheme for entanglement generation, as shown below. Giant atoms can be realized by using superconducting qubits [27, 31] or Rydberg atoms [32]. A

series of interesting phenomena for giant atoms have been already investigated, including frequency-dependent relaxation rate and Lamb shift [33], decoherence-free interaction between two giant atoms [34–36], oscillating bound states [37, 38] and long-lived entangled states [27, 39, 40].

In this Letter, we theoretically explore the generation and optimization of entanglement between giant atoms chirally coupled to 1D finite spin chains, acting as *spin cavities*, as shown schematically in Fig. 1(a). Following the steps of Ref. [12], magnons in these spin chains take the role of photons in standard optical cavities. Up to date, most theoretical and experimental studies have focused on giant atoms that are coupled to waveguides. It is known that entanglement can be greatly enhanced by strongly coupling matter excitations to cavity ones [6], so it is natural to ask whether there is an advantage for entanglement generation in coupling giant atoms to cavities. We examine the degree of entanglement by measuring the concurrence [41, 42], and employ the variational matrix product state (MPS) algorithm [43–48] to create a complete map of entanglement generation. Notice that, within the MPS approach, it is not necessary to restrict the Hilbert space to the single-excitation subspace. We study the effect of cavity length and chirality, revealing that small-size cavities chirally coupled to giant atoms can improve and expedite the generation of entanglement. Second, we consider applying a classical driving field on one of the giant atoms to create entanglement, finding out that maximal concurrence does not increase monotonically as a function of driving strength. To extend our study to more practical situations, we also consider the effect of disorder of the spin cavity sites on the entanglement. Although, as expected, disorder leads to a lower concurrence, large values of the concurrence

* you_jiabin@ihpc.a-star.edu.sg

† f.j.garcia@uam.es

can still be achieved even for scenarios presenting strong disorder. Enlightened by this study, we finally consider leveraging “disorder” in the cavity to both maximize the degree of entanglement and expedite the generation time, showing that a higher concurrence can be achieved within a shorter period of time when either the on-site energies or the hoppings in the cavity are properly tuned.

Model.— We consider entanglement generation between giant atoms that are coupled to a spin cavity at multiple points, as shown in Fig. 1(a). A series of N two-level systems describe the giant atoms, and the interaction between them is mediated by magnons excited within the spin cavity, which consists of a finite collection of N_c spin sites. The Hamiltonian for the whole system is given by $H = \sum_{i=1}^{N_T} \Delta_i \sigma_i^+ \sigma_i^- + \Omega_i (\sigma_i^+ + \sigma_i^-) + \sum_{i=1}^{N_T-1} (J_{1,i}^* \sigma_i^+ \sigma_{i+1}^- + J_{1,i} \sigma_{i+1}^+ \sigma_i^-) + \sum_{i=1}^{N_T-2} (J_{2,i}^* \sigma_i^+ \sigma_{i+2}^- + J_{2,i} \sigma_{i+2}^+ \sigma_i^-)$, where $N_T = N_c + N$, σ_i^\pm are the raising and lowering operators for both spins and two-level atoms, Δ_i and Ω_i are the on-site energy and the driving strength, respectively. For the sake of simplicity, in this work we analyze the case of just two giant atoms, placed at positions n_1 and n_2 . We consider a chiral coupling between them and the cavity by setting the nearest neighbor hopping as $J_{1,n_1-1} = J_{1,n_1} = A_{n_1} e^{-i\phi_{n_1}}$ and $J_{1,n_2-1} = J_{1,n_2} = A_{n_2} e^{-i\phi_{n_2}}$. Here the degree of chirality is introduced by a hopping phase ϕ_i , which is the Lamb shift acquired between neighboring coupling points for atom i [33]. We assume a non-chiral coupling between spins, $J_{1,i} = J$, and, to be consistent with the notation, we include a next nearest neighbor interaction, $J_{2,i}$, to account for the interaction between the two spins that are coupled to the giant atoms, $J_{2,n_1-1} = J_{2,n_2-1} = J$, $J_{2,i} = 0$ otherwise. The dissipation from the system to the environment can be described by the Lindblad master equation ($\hbar = 1$),

$$\frac{d\rho}{dt} = i[\rho, H] + \sum_{i=1}^{N_T} \frac{\Gamma_i}{2} \mathcal{D}[\sigma_i^-] \rho, \quad (1)$$

where ρ is the density matrix of the whole system and $\mathcal{D}[\sigma_i^-] \rho = 2\sigma_i^- \rho \sigma_i^+ - \sigma_i^+ \sigma_i^- \rho - \rho \sigma_i^+ \sigma_i^-$ is the Lindblad dissipator with decay rate Γ_i .

Effect of cavity length and chirality.— We first investigate the effect of cavity length and chirality on the concurrence, which is a measure of the degree of entanglement, varying between $C = 1$ (maximum entanglement) and $C = 0$ (no entanglement). Please see the Supplemental Material (SM) for the definition of this physical magnitude [49]. The giant atoms are initially prepared in the excited state $|1\rangle$ for atom n_1 and in the ground state $|0\rangle$ for atom n_2 , and there is no external driving ($\Omega_i = 0$). We plot the concurrence versus time and cavity length N_c in Fig. 1(b) for a particular chirality ($\phi_{n_1} = \phi_{n_2} = \pi/4$), observing a zero-concurrence region in the leftmost part of the panel that indicates ballistic propagation of excitation at short times. Increasing the cavity length from $N_c = 5$ to $N_c = 50$ delays the generation time and, furthermore, concurrence oscillates during the time evolu-

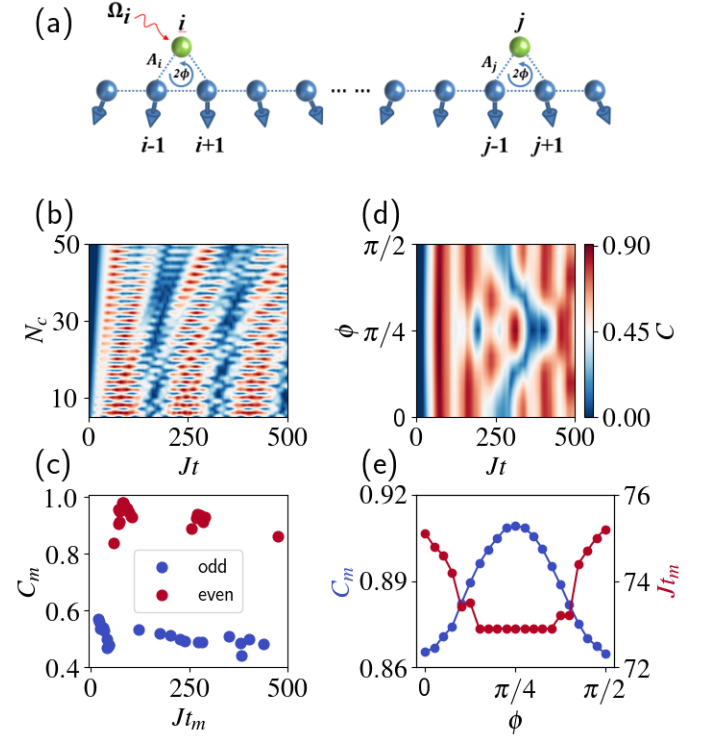


FIG. 1. (a) Schematic of driven giant atoms coupled to a spin cavity. Panel (b) renders the concurrence versus both time and N_c (from 5 to 50), whereas panel (c) shows the maximal concurrence, C_m , and the corresponding time t_m (in units of $1/J$) for the cases analyzed in (a). In these simulations $n_1 = 3$ and $n_2 = N_c$, and the coupling phases for the giant atoms n_1 and n_2 are $\phi_{n_1} = \phi_{n_2} = \pi/4$. Panels (d) and (e) illustrate the effect of chirality while the number of spins is fixed to $N_c = 50$: (d) concurrence versus hopping phase, $\phi_{n_1} = \phi_{n_2} = \phi$, and time, and (e) C_m (blue line) and Jt_m (red line) versus the hopping phase. Notice that panel (b) and panel (d) share the same colorbar. The amplitude is $A/J = 0.1$ and no dissipation is present, $\Gamma_i/J = 0$. The bond dimension $D = 10$ is used for the MPS simulations.

tion. Fig. 1(c) shows the maximum concurrence C_m and the corresponding optimal time, Jt_m , for different cavity lengths. We find that cavities presenting an odd number of spins result in low concurrence ($C_m < 0.6$), while even numbers lead to high concurrence ($C_m > 0.8$) scenarios. The maximum concurrence C_m of approximately 0.98 occurs for $N_c = 10$. Information on the optimum system size, N_T , associated with each point, can be found in the SM [49].

We then study the effect of chirality by analyzing the dependence of the concurrence with the coupling phase ϕ for a fixed cavity length, $N_c = 50$, and for an even distance between atoms, $\Delta n = n_2 - n_1 = 46$, as shown in Fig. 1(d). When the phase changes from 0 to $\pi/4$, it shifts the concurrence peak to a later time, except for the first peak. Notice also that the pattern is symmetric with respect to $\pi/4$. Fig. 1(e) shows that chiral coupling results in higher entanglement within a shorter time than

symmetric coupling. As shown in the SM, chirality has no significant effect on the concurrence dynamics for the case of odd distance between two giant atoms. Also in the SM we analyze the effect of dissipation on entanglement [49]. Our results then indicate that a small, even-sized cavity displaying a $\phi = \pi/4$ chiral atom-cavity coupling seems to be optimal for obtaining a higher concurrence between two giant atoms.

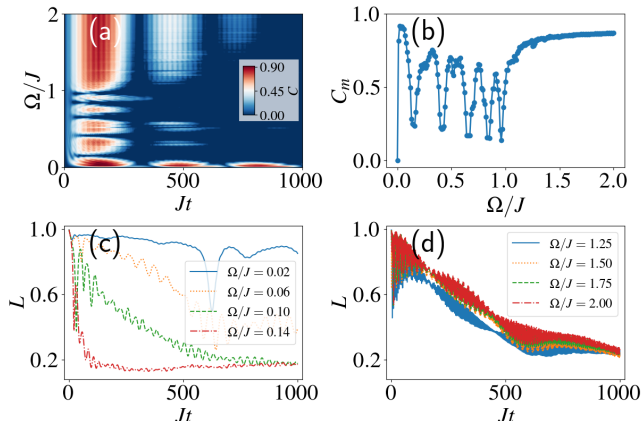


FIG. 2. Effect of driving on the concurrence. The parameters are $N_c = 10$, $n_1 = 3$, $n_2 = 10$, $A/J = 0.1$ and $\phi = \pi/4$. The on-site energies and the hopping amplitudes are the same as those in Fig. 1 and no dissipation, $\Gamma_{1\sim 12}/J = 0$, is included. (a) Concurrence versus time and driving Ω/J ; (b) maximal concurrence versus driving Ω/J ; (c) and (d) ratio of giant atom excitation to the total excitation, L , versus time, Jt , in the weak (panel c) and ultrastrong driving regimes (panel d).

Effect of driving.— In light of previous findings, we focus now on an even-sized spin cavity with number $N_c = 10$, chirally-coupled ($\phi = \pi/4$) to two giant atoms located at $n_1 = 3$ and $n_2 = 10$. We assume that the atom n_1 is driven by a classical driving field with strength Ω . The coupling strength between the cavity and the atoms is set to $A/J = 0.1$ and the on-site energies and hopping amplitudes are the same as those in Fig. 1. Here, as a difference with the case analyzed in Fig. 1, we consider that both atoms are in their ground states at $t = 0$. Our results in Fig. 2(a) reveal that entanglement dynamically evolves showing revival-and-death phenomena, with decreasing concurrence in each oscillatory lobe. When looking at the maximum concurrence for a given driving strength Ω (Fig. 2(b)), we find that for certain driving strengths smaller than J , entanglement cannot reach its maximum value, exhibiting an oscillating behaviour as a function of Ω . Surprisingly, the best entanglement scenario occurs at very weak driving strength ($C_m \approx 0.92$ at $\Omega/J = 0.02$). As the driving strength increases beyond J , the maximal concurrence gradually saturates to a large value, which is nevertheless lower than that obtained for weak driving. In Fig. 2(c) and 2(d), we use the ratio of giant atom excitation to the total excitation, defined as $L = \sum_{i=n_1, n_2} \sigma_i^+ \sigma_i^- / \sum_{i=1}^{N_T} \sigma_i^+ \sigma_i^-$ to measure the excitation leakage from the giant atom subsystem to the spin

cavity. It is found that the less the leakage, the higher the concurrence, which is exemplified by the case of driving $\Omega/J = 0.02$ in Fig. 2(c). Please also refer to SM for the details of total and giant-atom subsystem excitations [49]. In the weak driving limit ($\Omega/J \lesssim 0.1$), we find that as the driving strength increases, the leakage becomes significant, leading to a low concurrence regime shown in Fig. 2(b). This observation also applies to the oscillatory behaviour in the strong driving regime ($0.1 \lesssim \Omega/J \lesssim 1$). In the ultrastrong driving regime ($\Omega/J \gtrsim 1$), we find in Fig. 2(d) that the decrease of leakage in time are slower than the weak driving regime, leading to a stable concurrence pattern ($\Omega/J \gtrsim 1$), as shown in Fig. 2(a). Our findings provide deep insights into the intricate and non-trivial interplay between driving and entanglement generation, showing that a weak external driving leads to a higher entanglement.

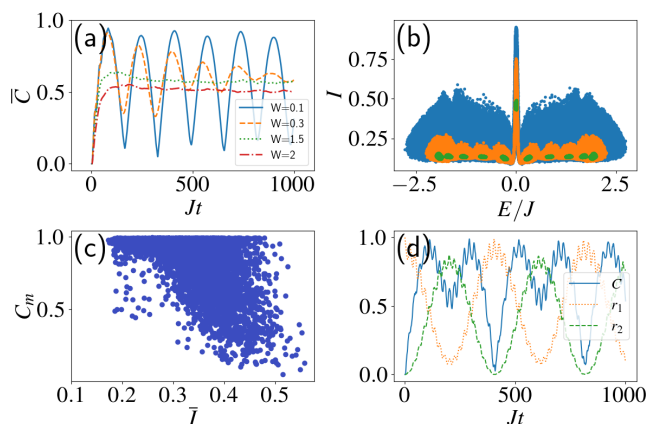


FIG. 3. Effect of disorder on the concurrence. (a) Average concurrence over 1000 random realizations for each value of W , $W = 0.1, 0.3, 1.5, 2$. (b) IPR of the eigenstates within the single excitation Hamiltonian versus its energy for $W = 0.1$ (green), 0.4 (orange), 1 (blue). In this case 10^5 realizations have been performed for each W . (c) Maximal concurrence versus average IPR for all the realizations in panel (a). (d) Concurrence dynamics and return probabilities for atoms n_1 (r_1) and n_2 (r_2) for a particular realization with disorder $W = 1$. The on-site energies are $\Delta_i/J = [-0.71, 0.86, 0.00, 0.19, 0.42, 0.50, -0.24, 0.19, -0.45, 0.00, 0.18, -1.00]$.

Effect of disorder.— Now we investigate the effect of disorder in the spin cavity on the entanglement generation. In previous calculations, we set that the two giant atoms were resonant with on-site energies, $\Delta_{n_1} = \Delta_{n_2} = 0$, but we now assume that the on-site energies of the cavity spins are randomly distributed in a given energy interval, $\Delta_i/J \in [-W, W]$, ($i \neq n_1, n_2$). The atom n_1 is initially prepared in state $|1\rangle$, whereas the atom n_2 and all the cavity spins are in the ground state $|0\rangle$. The other parameters are the same as those utilized in Fig. 1. In Fig. 3(a), we analyze the evolution of average concurrence \bar{C} for different disorder strengths W . It is found that, as expected, the average concurrence \bar{C} is gradually decreased as the disorder strength W increases.

When studying localization phenomena [50], it is standard to analyse the so-called inverse participation ratio (IPR), defined in our case as $I_j = \sum_{i=1}^{N_T} |c_i^j|^4$, c_i^j being the i -th component of the j -th eigenstate. This quantity measures the spatial spreading of the collective wavefunction and, as a simple rule, the higher the IPR, the more localized the wavefunction is and vice versa. In Fig. 3(b), we plot the IPR of the eigenstate of the single excitation Hamiltonian versus energy for three different disorder strengths. Please refer to SM for the details of single excitation Hamiltonian [49]. It is found that for weak disorder strengths ($W = 0.1$, green), most of the wavefunctions are delocalized except those with energies near the atoms' energy ($\Delta_{n_1} = \Delta_{n_2} = 0$). These wavefunctions are more localized to close the band gap and mediate the two giant atoms for generating entanglement. However, as the disorder strength increases, the energy gap closes (from green to orange) and states become more localized. Surprisingly, even for strong disorder ($W = 1$), we can still observe particular eigenstates presenting a delocalized character, i.e., low IPR, which is good for entangling two giant atoms. In Fig. 3(c), we render the maximal concurrence C_m versus average IPR ($\bar{I} = \sum I_j/N_T$), showing a decreasing trend in maximal concurrence for increasing IPR, as expected. It is found that higher concurrence ($C_m > 0.5$) is prone to happen in the lower \bar{I} systems ($\bar{I} < 0.35$). Furthermore, another criterion for generating high entanglement in disordered systems is the effective exchange of return probabilities for atom n_i , given by $r_i = |\langle 00 \cdots 1_{n_i} \cdots 00 | \psi(t) \rangle|^2$ ($i = 1, 2$). In Fig. 3(d), we show the time evolution of the concurrence (blue line) for a particular disorder realization corresponding to $W = 1$ and $\bar{I} = 0.23$, along with r_1 (orange dotted line) and r_2 (green dotted line). Notice that, even for this case in which disorder is very strong, maximum entanglement (around 0.99) occurs when $r_1 \approx r_2$ and minimum when r_1 and r_2 differ by a large value.

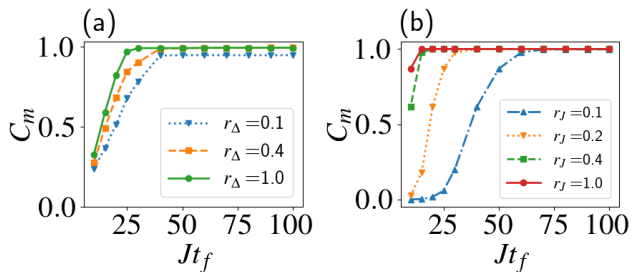


FIG. 4. Fast entanglement generation by engineering the on-site energies and hoppings. The number of cavity spins is $N_c = 10$. The two giant atoms are located at $n_1 = 3$ and $n_2 = 10$. Initially, atom n_1 is excited to state $|1\rangle$, while atom n_2 is in the ground state $|0\rangle$. All the cavity spins remain in the ground state. Maximal concurrence versus stopping time, Jt_f , for different restrictions for the engineering of on-site energies, r_Δ , in panel (a), and hoppings, r_J , in panel (b).

Fast entanglement generation.— In the previous sec-

tion, we have found that disorder can affect entanglement generation and that the average IPR can be used to measure the expected degree of entanglement. Here we propose a fast, high concurrence entanglement generation by engineering either the on-site energies or the hoppings in the cavity. We aim at maximizing the concurrence within a time interval $[0, Jt_f]$ where Jt_f is the stopping time in time evolution. When engineering the on-site energies, we restrict their values to the range $[-r_\Delta, r_\Delta]$ by setting $\Delta_i = r_\Delta \cos(\theta_i)$, the hoppings being the same as those in Fig. 1, whereas when tuning the hoppings, we restrict the hoppings to the range $[0, r_J]$ by setting $J_{1(2),i} = r_J \cos^2(\theta_{1(2),i}/2)$ and the on-site energies are the same as those in Fig. 1. In this way, the maximal concurrence within the time interval $[0, Jt_f]$ is then a function of angles, $C_m(\{\theta_i\})$ or $C_m(\{\theta_{1(2),i}\})$. In Fig. 4 we render the results of this optimization process for the two different scenarios by using the so-called **Powell** method, as implemented in the **SciPy** package. When compared with the homogeneous case discussed in Fig. 1, we find that by engineering either the on-site energies (panel a) or hoppings (panel b), high concurrence entanglement generation can be strongly accelerated. In Fig. 4(a) and 4(b), we show that with the increase of $r_{\Delta(J)}$, the two giant atoms can reach high concurrences ($C_m > 0.95$) within a shorter stopping time Jt_f compared with the homogeneous system. A detailed account of the parameters for achieving this improved performance in entanglement generation can be found in the SM [49]. It is important to highlight that compared to the time-dependent optimal control schemes previously proposed [51–53], our platform achieves a very high degree of entanglement without relying on any complex control of the fields and, therefore, is easier to implement experimentally, for example, by the IBM quantum device, IBM QX20 Tokyo [54–56], as detailed in the SM [49].

Conclusions.— We have explored the generation and optimization of entanglement between two giant atoms chirally coupled to a spin cavity. When analyzing the effect of cavity length and chirality in these platforms, we have found that small-sized cavities with an optimal chiral atom-cavity coupling leads to a high and fast entanglement generation between the two giant atoms. When an external classical driving field is applied, the system displays an oscillatory behaviour for the maximal concurrence, and maximum entanglement emerges for weak drivings. We also consider the effect of disorder in the spin cavity on entanglement generation and, as expected, we find that most of the disorder setups lead to lower concurrence as the disorder strength increases. However, it is possible to identify particular configurations that present a high concurrence entanglement even for strong disorder strength. Finally, we have demonstrated that by engineering the on-site energies or hoppings in the spin cavity, we can achieve a higher concurrence, larger than 0.999, which emerges at a shorter time (3-4 times faster) when compared to the homogeneous case.

The IHPC A*STAR Team acknowledges support from

the National Research Foundation Singapore (NRF2021-

QEP2-02-P01), A*STAR Career Development Award (C210112010), and A*STAR (C230917003, C230917007).

-
- [1] C. H. Bennett, G. Brassard, C. Crépeau, R. Jozsa, A. Peres, and W. K. Wootters, Teleporting an unknown quantum state via dual classical and einstein-podolsky-rosen channels, *Phys. Rev. Lett.* **70**, 1895 (1993).
- [2] A. K. Ekert, Quantum cryptography based on bell's theorem, *Phys. Rev. Lett.* **67**, 661 (1991).
- [3] F. Grosshans, G. Van Assche, J. Wenger, R. Brouri, N. J. Cerf, and P. Grangier, Quantum key distribution using gaussian-modulated coherent states, *Nature* **421**, 238 (2003).
- [4] T. M. Graham, Y. Song, J. Scott, C. Poole, L. Phuttitarn, K. Jooya, P. Eichler, X. Jiang, A. Marra, B. Grinmeyer, M. Kwon, M. Ebert, J. Cherek, M. T. Lichtman, M. Gillette, J. Gilbert, D. Bowman, T. Ballance, C. Campbell, E. D. Dahl, O. Crawford, N. S. Blunt, B. Rogers, T. Noel, and M. Saffman, Multi-qubit entanglement and algorithms on a neutral-atom quantum computer, *Nature* **604**, 457 (2022).
- [5] A. Gonzalez-Tudela, D. Martin-Cano, E. Moreno, L. Martin-Moreno, C. Tejedor, and F. J. Garcia-Vidal, Entanglement of two qubits mediated by one-dimensional plasmonic waveguides, *Phys. Rev. Lett.* **106**, 020501 (2011).
- [6] J. M. Raimond, M. Brune, and S. Haroche, Manipulating quantum entanglement with atoms and photons in a cavity, *Rev. Mod. Phys.* **73**, 565 (2001).
- [7] A. Blais, A. L. Grimsmo, S. M. Girvin, and A. Wallraff, Circuit quantum electrodynamics, *Rev. Mod. Phys.* **93**, 025005 (2021).
- [8] M. H. Goerz, G. Gualdi, D. M. Reich, C. P. Koch, F. Motzoi, K. B. Whaley, J. Vala, M. M. Müller, S. Montangero, and T. Calarco, Optimizing for an arbitrary perfect entangler. ii. application, *Physical Review A* **91**, 062307 (2015).
- [9] P. Watts, J. Vala, M. M. Müller, T. Calarco, K. B. Whaley, D. M. Reich, M. H. Goerz, and C. P. Koch, Optimizing for an arbitrary perfect entangler. i. functionals, *Physical Review A* **91**, 062306 (2015).
- [10] M. M. Müller, D. M. Reich, M. Murphy, H. Yuan, J. Vala, K. Whaley, T. Calarco, and C. Koch, Optimizing entangling quantum gates for physical systems, *Physical Review A* **84**, 042315 (2011).
- [11] H. Pichler, T. Ramos, A. J. Daley, and P. Zoller, Quantum optics of chiral spin networks, *Physical Review A* **91**, 042116 (2015).
- [12] T. Ramos, B. Vermersch, P. Hauke, H. Pichler, and P. Zoller, Non-markovian dynamics in chiral quantum networks with spins and photons, *Phys. Rev. A* **93**, 062104 (2016).
- [13] T. Ramos, H. Pichler, A. J. Daley, and P. Zoller, Quantum spin dimers from chiral dissipation in cold-atom chains, *Physical review letters* **113**, 237203 (2014).
- [14] P. Lodahl, S. Mahmoodian, S. Stobbe, A. Rauschenbeutel, P. Schneeweiss, J. Volz, H. Pichler, and P. Zoller, Chiral quantum optics, *Nature* **541**, 473 (2017).
- [15] K. Kleinbeck, H. Busche, N. Stiesdal, S. Hofferberth, K. Mølmer, and H. P. Büchler, Creation of nonclassical states of light in a chiral waveguide, *Physical Review A* **107**, 013717 (2023).
- [16] C. Gonzalez-Ballester, A. Gonzalez-Tudela, F. J. Garcia-Vidal, and E. Moreno, Chiral route to spontaneous entanglement generation, *Physical Review B* **92**, 155304 (2015).
- [17] W.-K. Mok, J.-B. You, L.-C. Kwek, and D. Aghamalyan, Microresonators enhancing long-distance dynamical entanglement generation in chiral quantum networks, *Phys. Rev. A* **101**, 053861 (2020).
- [18] W.-K. Mok, D. Aghamalyan, J.-B. You, T. Haug, W. Zhang, C. E. Png, and L.-C. Kwek, Long-distance dissipation-assisted transport of entangled states via a chiral waveguide, *Phys. Rev. Research* **2**, 013369 (2020).
- [19] J. Petersen, J. Volz, and A. Rauschenbeutel, Chiral nanophotonic waveguide interface based on spin-orbit interaction of light, *Science* **346**, 67 (2014).
- [20] A. B. Young, A. C. T. Thijssen, D. M. Beggs, P. Androvitsaneas, L. Kuipers, J. G. Rarity, S. Hughes, and R. Oulton, Polarization engineering in photonic crystal waveguides for spin-photon entanglers, *Phys. Rev. Lett.* **115**, 153901 (2015).
- [21] J. Lin, J. P. B. Mueller, Q. Wang, G. Yuan, N. Antoniou, X.-C. Yuan, and F. Capasso, Polarization-controlled tunable directional coupling of surface plasmon polaritons, *Science* **340**, 331 (2013).
- [22] K. Stannigel, P. Rabl, A. S. Sørensen, M. D. Lukin, and P. Zoller, Optomechanical transducers for quantum information processing, *Phys. Rev. A* **84**, 042341 (2011).
- [23] G. Yang, C.-H. Hsu, P. Stano, J. Klinovaja, and D. Loss, Long-distance entanglement of spin qubits via quantum hall edge states, *Phys. Rev. B* **93**, 075301 (2016).
- [24] M. V. Gustafsson, T. Aref, A. Frisk Kockum, M. K. Ekström, G. Johansson, and P. Delsing, Propagating phonons coupled to an artificial atom, *Science* **346**, 207 (2014).
- [25] R. Manenti, A. F. Kockum, A. Patterson, T. Behrle, J. Rahamim, G. Tancredi, F. Nori, and P. J. Leek, Circuit quantum acoustodynamics with surface acoustic waves, *Nature Communications* **8**, 975 (2017).
- [26] B. A. Moores, L. R. Sletten, J. J. Viennot, and K. W. Lehnert, Cavity quantum acoustic device in the multimode strong coupling regime, *Phys. Rev. Lett.* **120**, 227701 (2018).
- [27] B. Kannan, M. J. Ruckriegel, D. L. Campbell, A. Frisk Kockum, J. Braumüller, D. K. Kim, M. Kjaergaard, P. Krantz, A. Melville, B. M. Niedzielski, A. Vepsäläinen, R. Winik, J. L. Yoder, F. Nori, T. P. Orlando, S. Gustavsson, and W. D. Oliver, Waveguide quantum electrodynamics with superconducting artificial giant atoms, *Nature* **583**, 775 (2020).
- [28] A. M. Vadiraj, A. Ask, T. G. McConkey, I. Nsanzineza, C. W. S. Chang, A. F. Kockum, and C. M. Wilson, Engineering the level structure of a giant artificial atom in waveguide quantum electrodynamics, *Phys. Rev. A* **103**, 023710 (2021).
- [29] Y.-T. Chen, L. Du, L. Guo, Z. Wang, Y. Zhang, Y. Li,

- and J.-H. Wu, Nonreciprocal and chiral single-photon scattering for giant atoms, *Communications Physics* **5**, 215 (2022).
- [30] A. Soro and A. F. Kockum, Chiral quantum optics with giant atoms, *Phys. Rev. A* **105**, 023712 (2022).
- [31] X. Wang and H.-R. Li, Chiral quantum network with giant atoms, *Quantum Science and Technology* **7**, 035007 (2022).
- [32] Y.-T. Chen, L. Du, Y. Zhang, L. Guo, J.-H. Wu, M. Artoni, and G. C. La Rocca, Giant-atom effects on population and entanglement dynamics of rydberg atoms in the optical regime, *Phys. Rev. Res.* **5**, 043135 (2023).
- [33] A. Frisk Kockum, P. Delsing, and G. Johansson, Designing frequency-dependent relaxation rates and lamb shifts for a giant artificial atom, *Phys. Rev. A* **90**, 013837 (2014).
- [34] A. F. Kockum, G. Johansson, and F. Nori, Decoherence-free interaction between giant atoms in waveguide quantum electrodynamics, *Phys. Rev. Lett.* **120**, 140404 (2018).
- [35] A. Carollo, D. Cilluffo, and F. Ciccarello, Mechanism of decoherence-free coupling between giant atoms, *Phys. Rev. Res.* **2**, 043184 (2020).
- [36] A. Soro, C. S. Muñoz, and A. F. Kockum, Interaction between giant atoms in a one-dimensional structured environment, *Phys. Rev. A* **107**, 013710 (2023).
- [37] K. H. Lim, W.-K. Mok, and L.-C. Kwek, Oscillating bound states in non-markovian photonic lattices, *Phys. Rev. A* **107**, 023716 (2023).
- [38] L. Guo, A. F. Kockum, F. Marquardt, and G. Johansson, Oscillating bound states for a giant atom, *Phys. Rev. Res.* **2**, 043014 (2020).
- [39] A. C. Santos and R. Bachelard, Generation of maximally entangled long-lived states with giant atoms in a waveguide, *Phys. Rev. Lett.* **130**, 053601 (2023).
- [40] X.-L. Yin and J.-Q. Liao, Generation of two-giant-atom entanglement in waveguide-qed systems, *Phys. Rev. A* **108**, 023728 (2023).
- [41] W. K. Wootters, Entanglement of formation and concurrence., *Quantum Inf. Comput.* **1**, 27 (2001).
- [42] R. Horodecki, P. Horodecki, M. Horodecki, and K. Horodecki, Quantum entanglement, *Rev. Mod. Phys.* **81**, 865 (2009).
- [43] U. Schollwöck, The density-matrix renormalization group in the age of matrix product states, *Ann. Phys. (N. Y.)* **326**, 96 (2011).
- [44] F. Verstraete, V. Murg, and J. Cirac, Matrix product states, projected entangled pair states, and variational renormalization group methods for quantum spin systems, *Adv. Phys.* **57**, 143 (2008).
- [45] J. Cui, J. I. Cirac, and M. C. Bañuls, Variational matrix product operators for the steady state of dissipative quantum systems, *Phys. Rev. Lett.* **114**, 220601 (2015).
- [46] J.-B. You, X. Xiong, P. Bai, Z.-K. Zhou, W.-L. Yang, C. E. Png, L. C. Kwek, and L. Wu, Suppressing decoherence in quantum plasmonic systems by the spectral-hole-burning effect, *Phys. Rev. A* **103**, 053517 (2021).
- [47] J. Haegeman, J. I. Cirac, T. J. Osborne, I. Pižorn, H. Verschelde, and F. Verstraete, Time-dependent variational principle for quantum lattices, *Phys. Rev. Lett.* **107**, 070601 (2011).
- [48] J. Haegeman, C. Lubich, I. Oseledets, B. Vandereycken, and F. Verstraete, Unifying time evolution and optimization with matrix product states, *Phys. Rev. B* **94**, 165116 (2016).
- [49] See Supplemental Material at [URL] for further details of 1) the definition of concurrence; 2) information on the optimum system size, associated with each point; 3) effects of chirality and dissipation; 4) total and giant-atom subsystem excitations under a classical driving field; 5) the definition of single excitation Hamiltonian; 6) the parameters for achieving improved performance in entanglement generation; 7) experimental realization of our proposal.
- [50] P. W. Anderson, Absence of diffusion in certain random lattices, *Phys. Rev.* **109**, 1492 (1958).
- [51] F. Motzoi, J. M. Gambetta, P. Rebentrost, and F. K. Wilhelm, Simple pulses for elimination of leakage in weakly nonlinear qubits, *Phys. Rev. Lett.* **103**, 110501 (2009).
- [52] X. Li, X. Shao, and W. Li, Single temporal-pulse-modulated parameterized controlled-phase gate for rydberg atoms, *Phys. Rev. Appl.* **18**, 044042 (2022).
- [53] J. M. Chow, L. DiCarlo, J. M. Gambetta, F. Motzoi, L. Frunzio, S. M. Girvin, and R. J. Schoelkopf, Optimized driving of superconducting artificial atoms for improved single-qubit gates, *Phys. Rev. A* **82**, 040305 (2010).
- [54] V. Gheorghiu, J. Huang, S. M. Li, M. Mosca, and P. Mukhopadhyay, Reducing the cnot count for clifford+t circuits on nisq architectures, *IEEE Transactions on Computer-Aided Design of Integrated Circuits and Systems* **42**, 1873 (2020).
- [55] Y. Qian, Z. Guan, S. Zheng, and S. Feng, A method based on timing weight priority and distance optimization for quantum circuit transformation, *Entropy* **25** (2023).
- [56] T. G. de Brugière, M. Baboulin, B. Valiron, S. Martiel, and C. Allouche, Quantum cnot circuits synthesis for nisq architectures using the syndrome decoding problem, In: Lanese, I., Rawski, M. (eds) *Reversible Computation. RC 2020. Lecture Notes in Computer Science*, Springer, Cham. **12227**, 189 (2020).